The Astronomical Journal, 142:143 (2pp), 2011 October doi:10.1088/0004-6256/142/4/143

ERRATUM: "CORRELATIONS OF QUASAR OPTICAL SPECTRA WITH RADIO MORPHOLOGY" (2011, AJ, 141, 182)

Amy E. Kimball[1,2], Željko Ivezić[2], Paul J. Wiita[3,4], and Donald P. Schneider[5]
[1] National Radio Astronomy Observatory, 520 Edgemont Road, Charlottesville, VA 22903-2475, USA; akimball@nrao.edu
[2] Department of Astronomy, University of Washington, Box 351580, Seattle, WA 98195-1580, USA
[3] Department of Physics, The College of New Jersey, P.O. Box 7718, Ewing, NJ 08628, USA
[4] Department of Physics and Astronomy, Georgia State University, P.O. Box 4106, Atlanta, GA 30302-4106, USA
[5] Department of Astronomy and Astrophysics, Pennsylvania State University, 525 Davey Laboratory, University Park, PA 16802, USA
Received 2011 August 17; published 2011 September 16

Online-only material: color figures

Equation (3) in the published article contained a sign error, such that the two terms in the exponent were reversed. The correct version of the equation is

$$R = R_{[20\,\mathrm{cm}]} = \frac{S_{\mathrm{core}}}{S_{\mathrm{lobe}}}(1+z)^{(\alpha_{\mathrm{lobe}}-\alpha_{\mathrm{core}})}. \quad (3)$$

This correction only affects the published equation. The code that calculated the R values for the plots and analysis in the published article used the correct formula.

A separate error led to incorrect values in three rows of Table 8. Owing to an error in the software, the linear regression analysis was performed using the wrong abscissa values for the three rows corresponding to the *lobe* morphology class for equivalent width versus R. We provide the corrected table in its entirety below. None of the corrected linear regressions suggests a significant correlation; thus there is no change to the overall conclusions presented in the published article. This correction also affects the middle panels of Figures 12–14, which show the best-fit line for these sources. The figures are reproduced below with the corrected best-fit lines.

We are grateful to Dr. Neal Jackson for bringing these errors to our attention.

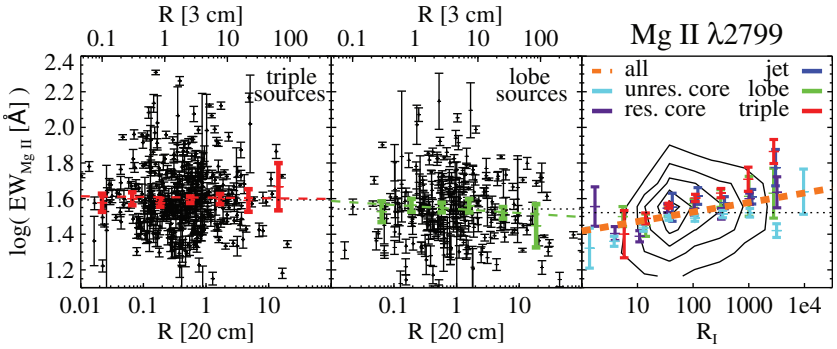

Figure 12. EW of Mg II λ2799 as a function of core-boosting parameters R and R_{I}. In the left and middle panels, the full distributions are shown as black points. In the right panel, the full distribution is shown as linearly spaced contours. The number of sources in each panel and each morphology class is listed in Table 8. To guide the eye, colored error bars show the median (and error in the median) EW in evenly spaced log(R) or log(R_{I}) bins. Horizontal dotted lines show the median value for each panel. Dashed lines show the best-fit line for the full set of sources in each panel. Quantitative results of the linear regression for all morphology classes are listed in Table 8.

(A color version of this figure is available in the online journal.)

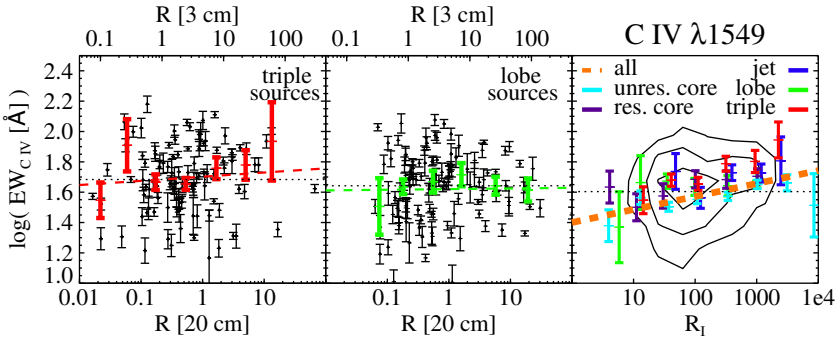

Figure 13. EW of C IV λ1549 as a function of core-boosting parameters R and R_{I}. Colors and symbols are the same as in Figure 12. Number of sources of each class and results of the linear regression analysis are listed in Table 8.

(A color version of this figure is available in the online journal.)

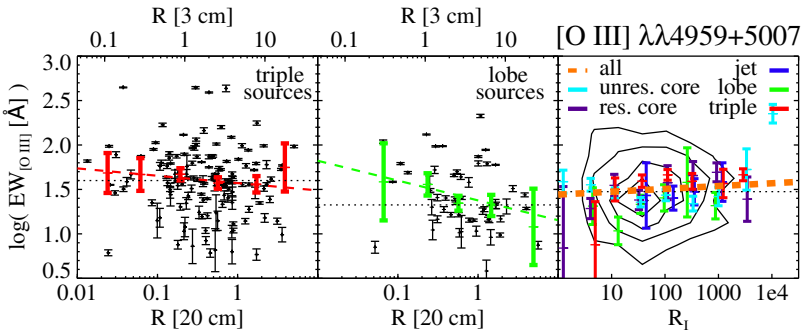

Figure 14. EW of [O III] λλ4959/5007 as a function of core-boosting parameters R and R_I. Colors and symbols are the same as in Figure 12. Number of sources of each class and results of the linear regression analysis are listed in Table 8.

(A color version of this figure is available in the online journal.)

Table 8
Linear Regression Results

Y	X	Class	Number of Sources	A	B	Pearson	Figure
EW Mg II	R	Lobe	261	$1.54^{+0.013}_{-0.012}$	$-0.023^{+0.017}_{-0.018}$	$-0.081^{+0.062}_{-0.061}$	12
		Triple	420	$1.61^{+0.011}_{-0.011}$	$-0.004^{+0.016}_{-0.015}$	$-0.012^{+0.052}_{-0.050}$	
		All radio	**2929**	$\mathbf{1.42^{+0.012}_{-0.011}}$	$\mathbf{0.053^{+0.005}_{-0.006}}$	$\mathbf{0.179^{+0.018}_{-0.018}}$	
		Unresolved core	**1602**	$\mathbf{1.42^{+0.015}_{-0.016}}$	$\mathbf{0.034^{+0.007}_{-0.008}}$	$\mathbf{0.112^{+0.024}_{-0.025}}$	
EW Mg II	R_I	**Resolved core**	**384**	$\mathbf{1.38^{+0.024}_{-0.024}}$	$\mathbf{0.070^{+0.012}_{-0.012}}$	$\mathbf{0.309^{+0.046}_{-0.050}}$	
		Jet	**126**	$\mathbf{1.33^{+0.073}_{-0.075}}$	$\mathbf{0.103^{+0.029}_{-0.028}}$	$\mathbf{0.332^{+0.087}_{-0.090}}$	
		Lobe	265	$1.48^{+0.040}_{-0.039}$	$0.032^{+0.020}_{-0.020}$	$0.096^{+0.062}_{-0.060}$	
		Triple	**491**	$\mathbf{1.41^{+0.032}_{-0.030}}$	$\mathbf{0.100^{+0.015}_{-0.015}}$	$\mathbf{0.294^{+0.042}_{-0.044}}$	
EW C IV	R	Lobe	119	$1.62^{+0.023}_{-0.022}$	$0.004^{+0.033}_{-0.034}$	$0.012^{+0.094}_{-0.097}$	13
		Triple	109	$1.70^{+0.022}_{-0.023}$	$0.028^{+0.030}_{-0.032}$	$0.090^{+0.102}_{-0.106}$	
		All radio	**1398**	$\mathbf{1.40^{+0.023}_{-0.023}}$	$\mathbf{0.086^{+0.011}_{-0.011}}$	$\mathbf{0.215^{+0.026}_{-0.026}}$	
		Unresolved core	**945**	$\mathbf{1.37^{+0.030}_{-0.030}}$	$\mathbf{0.082^{+0.014}_{-0.014}}$	$\mathbf{0.195^{+0.032}_{-0.033}}$	
EW C IV	R_I	**Resolved core**	**138**	$\mathbf{1.40^{+0.054}_{-0.054}}$	$\mathbf{0.111^{+0.026}_{-0.028}}$	$\mathbf{0.341^{+0.074}_{-0.082}}$	
		Jet	46	$1.63^{+0.111}_{-0.116}$	$0.034^{+0.043}_{-0.041}$	$0.139^{+0.170}_{-0.169}$	
		Lobe	119	$1.56^{+0.073}_{-0.079}$	$0.033^{+0.040}_{-0.036}$	$0.082^{+0.100}_{-0.090}$	
		Triple	**130**	$\mathbf{1.48^{+0.067}_{-0.067}}$	$\mathbf{0.110^{+0.032}_{-0.032}}$	$\mathbf{0.298^{+0.084}_{-0.084}}$	
EW [O III]	R	Lobe	60	$1.38^{+0.049}_{-0.050}$	$-0.223^{+0.079}_{-0.079}$	$-0.368^{+0.129}_{-0.121}$	14
		Triple	137	$1.57^{+0.041}_{-0.042}$	$-0.083^{+0.062}_{-0.059}$	$-0.116^{+0.087}_{-0.084}$	
		All radio	840	$1.44^{+0.037}_{-0.036}$	$0.032^{+0.019}_{-0.019}$	$0.059^{+0.035}_{-0.035}$	
		Unresolved core	436	$1.48^{+0.049}_{-0.050}$	$-0.003^{+0.027}_{-0.027}$	$-0.005^{+0.047}_{-0.049}$	
EW [O III]	R_I	Resolved core	125	$1.39^{+0.081}_{-0.084}$	$0.081^{+0.046}_{-0.047}$	$0.162^{+0.090}_{-0.094}$	
		Jet	32	$1.32^{+0.338}_{-0.338}$	$0.063^{+0.128}_{-0.132}$	$0.102^{+0.199}_{-0.215}$	
		Lobe	62	$1.34^{+0.159}_{-0.157}$	$0.032^{+0.088}_{-0.087}$	$0.052^{+0.138}_{-0.140}$	
		Triple	161	$1.45^{+0.104}_{-0.103}$	$0.078^{+0.050}_{-0.051}$	$0.127^{+0.078}_{-0.083}$	
		Radio-quiet	**21,067**	$\mathbf{9.40^{+0.153}_{-0.160}}$	$\mathbf{-0.257^{+0.005}_{-0.005}}$	$\mathbf{-0.336^{+0.006}_{-0.006}}$	
		All radio	**1388**	$\mathbf{9.61^{+0.720}_{-0.705}}$	$\mathbf{-0.264^{+0.023}_{-0.023}}$	$\mathbf{-0.294^{+0.025}_{-0.025}}$	
		Unresolved core	**937**	$\mathbf{9.18^{+0.901}_{-0.975}}$	$\mathbf{-0.251^{+0.032}_{-0.030}}$	$\mathbf{-0.268^{+0.033}_{-0.031}}$	
		Resolved core	**138**	$\mathbf{10.64^{+2.103}_{-2.021}}$	$\mathbf{-0.297^{+0.067}_{-0.069}}$	$\mathbf{-0.369^{+0.080}_{-0.081}}$	
EW C IV	L_ν(1549 Å)	Jet	45	$4.68^{+3.449}_{-3.417}$	$-0.098^{+0.113}_{-0.114}$	$-0.146^{+0.168}_{-0.167}$	
		Lobe	**118**	$\mathbf{9.16^{+2.055}_{-1.984}}$	$\mathbf{-0.248^{+0.066}_{-0.067}}$	$\mathbf{-0.342^{+0.091}_{-0.087}}$	
		Triple	**130**	$\mathbf{9.19^{+2.076}_{-2.025}}$	$\mathbf{-0.246^{+0.067}_{-0.068}}$	$\mathbf{-0.327^{+0.089}_{-0.089}}$	
		Double-lobe	87	$7.03^{+2.566}_{-2.643}$	$-0.180^{+0.087}_{-0.084}$	$-0.244^{+0.119}_{-0.111}$	

Note. Distributions with significant correlations are shown in bold text. We define a significant correlation as having slope B and correlation coefficient that are non-zero with at least 3σ certainty. We exclude statistical analysis for samples with fewer than 20 sources.